On the optical verification of the influence of the ignition on the regression surface of a cigarette-burning small-scale solid rocket motor

J Hijlkema, Q. Levard

ON THE OPTICAL VERIFICATION OF THE INFLUENCE OF THE IGNITION ON THE REGRESSION SURFACE OF A CIGARETTE-BURNING SMALL-SCALE SOLID ROCKET MOTOR

J. Hijlkema[1] **and Q. Levard**[1]

[1] *ONERA/DMPE, Université de Toulouse, F-31410 Mauzac, France*
jouke.hijlkema@onera.fr,quentin.levard@onera.fr

1 Nomenclature

D fuel grain diameter

H fuel grain height

P' fluctuating combustion chamber pressure

P_{ig} igniter pressure

$\bar{P}$ stationary combustion chamber pressure

$\bar{V}_r$ average regression rate

t_0 ignition instant

t_b burn time

t_d instant the burning surface hits the head end

t_p instant the pixel p turns white

LP8#03 Third LP8 run, first with the transparent head end

LP8#11 Eleventh LP8 run, second with the transparent head end

Abstract

This paper covers an innovative method to reconstruct the evolution of the topology of the regressing surface of a cigarette-burning solid propellant. The basic idea is to film the last instances of the burn through a transparent head end of an existing, small-scale, experimental motor.

The time-evolution of the luminescent topology from the moment the burning surface hits the front-end until the extinction of the motor allows for the reconstruction of the topology of the burning surface at the end of the burn. Under the hypothesis of a parallel regressing surface, it is possible to inverse the time-evolution of this surface up until the ignition phase and thus to reconstruct the complete burn.

This information is particularly useful to assess the influence of non-homogeneous ignition patterns and the propagation of these patterns during the run. The modifications applied to an existing experimental set-up as well as the obtained data and their analysis are presented.

2 Introduction

To study the dynamic response of a burning propergol to pressure fluctuations, an experimental, small scale test engine was first devised and tested in the 1960s [**barrere74:˙onera˙snpe**, **kuentzmann75:˙repon˙proper˙sol˙oscil˙press˙vites**, **traineau94:˙exper**, **cauty99:˙solid**, **vuillot1986flow**].

The engine, called LP8, consists of an extremely short, cylindrical combustion chamber containing a cylindrical propellant grain (cf. figure 1). The grain is inhibited on all faces except for the rear facing side. The idea behind this set up is to assure a constant combustion chamber pressure once the ignition transient has passed while limiting the acoustic pressure oscillations. The igniter is placed radially, slightly above the surface of the propellant grain. The nozzle has no divergence and the sonic throat is partially obstructed by a toothed wheel rotating at a constant speed chosen before the start of the experiment. This allows for the determination of both the stationary

combustion chamber pressure ($\bar{P}$) and the fluctuating combustion chamber pressure (P') under stable conditions while imposing the frequency of P' [**Carricart2022**].

It is clear that it is of prime importance to have a constant $\bar{P}$. This can only be obtained by a constant burning surface area and we therefor have to be sure that the pyrotechnic igniter does not dig a furrow in the originally flat surface during the ignition phase.

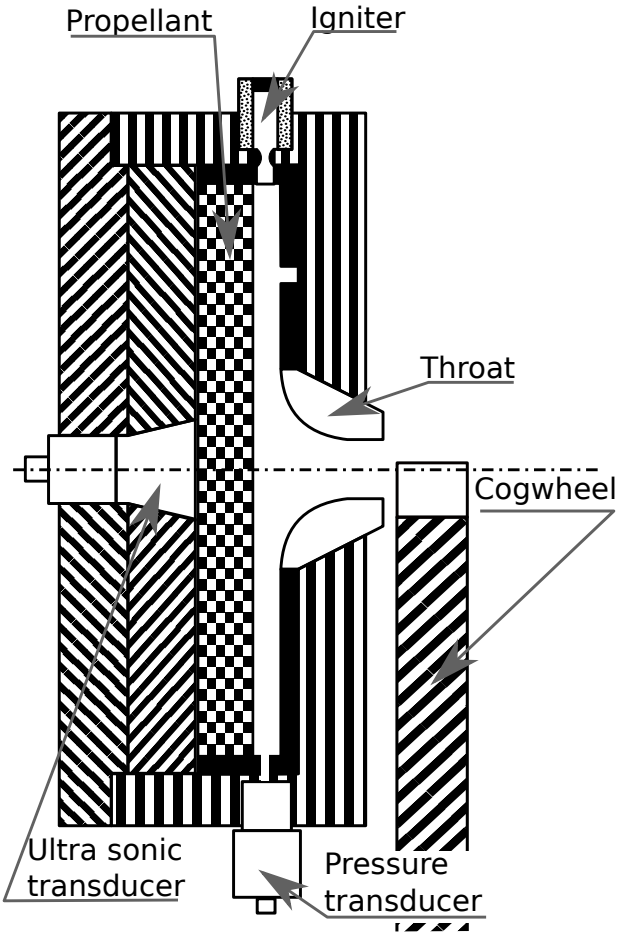

Figure 1: LP8 experimental set-up

In an ideal motor this would be easy to verify since a changing surface area would result in a change in $\bar{P}$ over time. However, this is not necessarily the case for real world experiments where heat losses, erosion or propellant inhomogeneities could mimic or counter act these variations. We therefor decided to try another approach and equipped our motor with a transparent head end so we could film the circumference of the fuel grain during operation as well as the end phase of the combustion where the head end gets uncovered as the propellant grain is fully consumed (see figure 2).

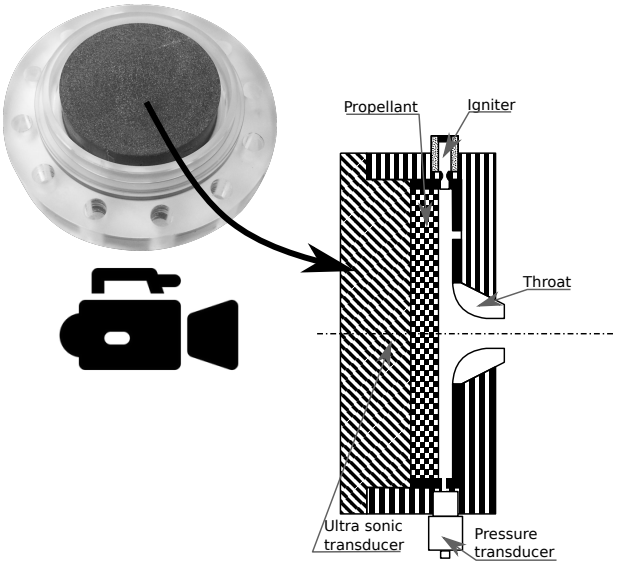

Figure 2: transparent head end set-up

The evolution of the frontier of the burning propergol is a measure of the “flatness” of the combustion surface. Ideally this evolution is infinitely fast as the perfectly parallel burning surface hits the head end of the combustion chamber.

Figure 3 shows two extreme ignition scenarios. On the left side the igniter digs a deep furrow in the propellant surface, the regression of the burning surface yields a variation of the area of the burning surface and leads to a typical uncovering of the transparent head end. This could result in an unacceptable variation of $\bar{P}$.

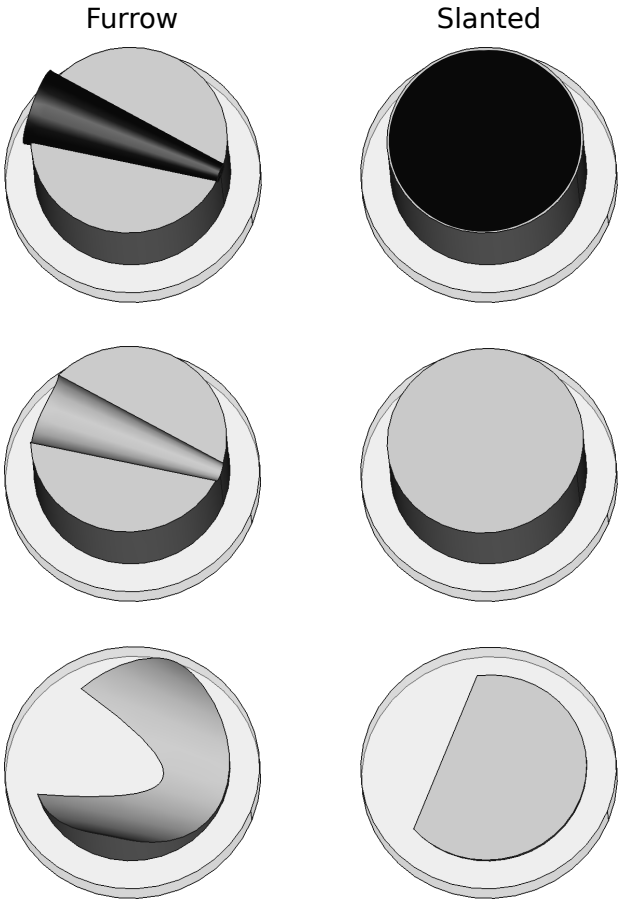

Figure 3: Ignition scenarios

The right side of the image shows no furrow but a slanting of the burning surface. This is acceptable since the burning surface area is constant over time. The slant angle will define the duration of the uncovering of the head end.

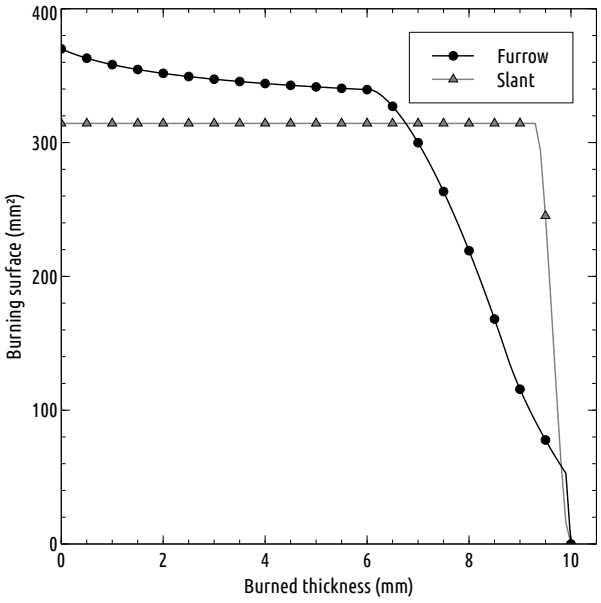

Figure 4: Evolution of the burning surface

Figure 4 shows the geometric evolution[1] of the area of the burning surface for two cases depicted above as a function of the burned thickness. The chamber pressure $\bar{P}$ is directly proportional to the area of the burning surface. So if the igniter does hollow the initially flat surface we should see a pressure curve that resembles the surface evolution as given in figure 4 and its traces must effect the way the head end uncovers.

3 Experimental set-up

4 Experimental results

We carried out two test runs with the transparent head end; LP8#03 with a standard igniter charge and LP8#11 with a beefed up igniter charge with the idea that we should see more of a furrow for LP8#11.

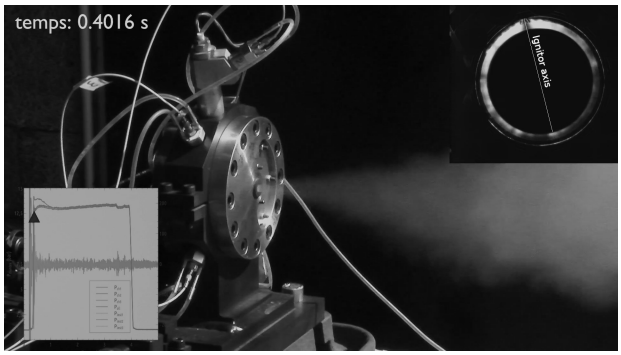

Figure 5: Ignition LP8.3

Figure 5 shows the ignition instant of the LP8#03. Bottom left shows the combined pressure curves ($\bar{P}$, P' and igniter pressure) with a black triangle indicating the instant. The top right shows the image captured with the high-speed camera through the transparent head end. The igniter axis is drawn as a white line.

Figure 6 shows the instant the burning surface hits the head end. We note a nice linear front starting from the side opposite of the igniter. This indicates that the grain was burning slightly slanted.

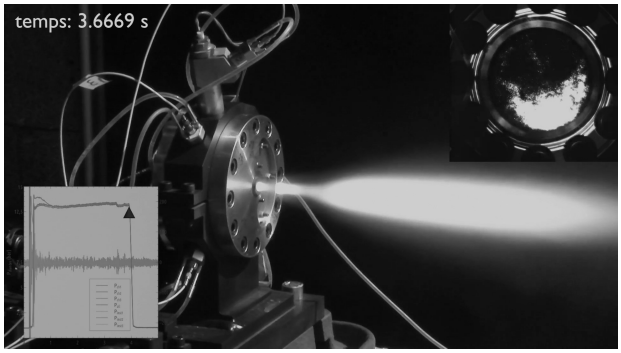

Figure 6: End phase LP8.3

4.1 Reconstruction method

The idea behind the reconstruction method is to use the visual information captured by the high-speed camera to reconstruct the topology of the burning surface just before the extinction of the motor. If this yields a relatively smooth surface (limited noise) than we can hope to be able to reverse time using the average regression rate and reconstruct the time evolution of the burning surface. If there is too much noise to we will need to fit the results with a smooth surface (based on a hypothetical surface shape at the ignition instant (t_0)) before reconstructing the time evolution.

If we assume that the average regression rate ($\bar{V}_r$) is constant during the burn and equal to $\bar{V}_r = \frac{H}{t_b}$ with H the fuel grain height and t_b the burn time. We take t_d to be the instant the first pixels become white (this is the moment the burning surface touches the transparent head end) and we record, for each pixel p the instant t_p it turns white, counting from t_d. Then, if the local angle between the burning surface and the head end surface is small, each pixel p with coordinates (x_p, y_p) corresponds with a point on the burning surface at instant t_d $c_p \approx (x_p, y_p, \bar{V}_r \times t_p)$.

If we apply this to the LP8#03 video we find the surface given in figure 7. The darker the colour the smaller t_p.

[1] Calculated with an in-house code based on the excellent opencascade libraries (`https://www.opencascade.com/`)

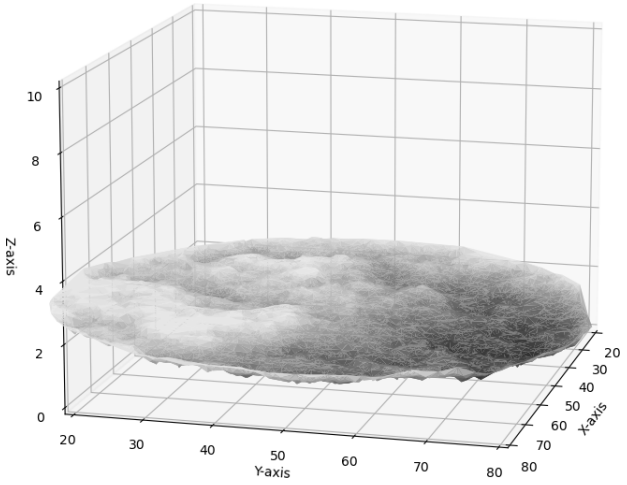

Figure 7: Reconstruction of the burning surface

A second, interesting, information we can extract from the video is the average light intensity per frame. We can imagine that the flame intensity is linked to the pressure through Veille's law $\bar{V}_r = aP^b$. The radiation of the gas that, apriori, is of constant composition, depends on the temperature and the pressure. The equilibrium temperature varies only slightly so the pressure dependence should be strong; higher pressure means more matter and therefor more radiation. If this hypothesis is correct then we should be able to deduce the pressure variations (not the absolute values) from the light intensity measurements.

4.2 LP8#03

Figure 8 shows the pressure measurements for LP8#03. We note that $t_b = 3.7$ s so, given that $H = 22.7$ mm we can deduce that $\bar{V}_r = 6.14$ mm/s. The reconstructed surface given in figure 7 is relatively flat but still too noisy to be used for the reconstruction.

If we use a least square method, the best fitting plane is $z = -0.008068x + -0.002351y + 1.133618$. So with $\bar{V}_r$=6.14 mm/s and D=81.5 mm we find,

$$t_b - t_d = D \times \frac{0.008068 + 0.002351}{\bar{V}_r} = 0.138 \text{ s}$$

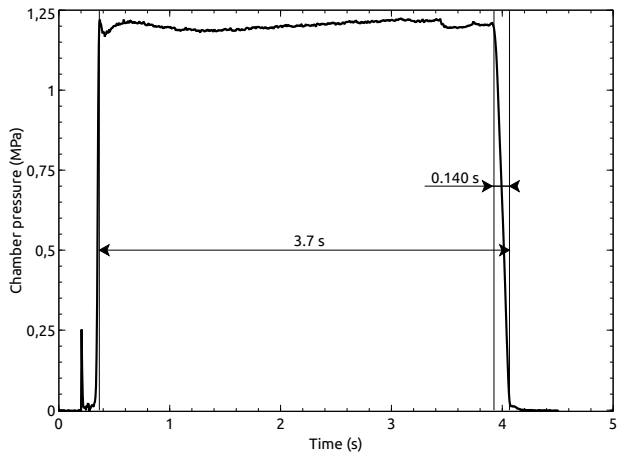

Figure 8: Pressure measurement LP8#03

This compares nicely with the measured 0.140 s given in figure 8.

Now, if we use our in-house tool mentioned in 1 to do the reverse regression of the best fitting plane we find the burning surface evolution given in figure 9. As expected the surface area is constant during the run and drops with a constant rate once discovery occurs.

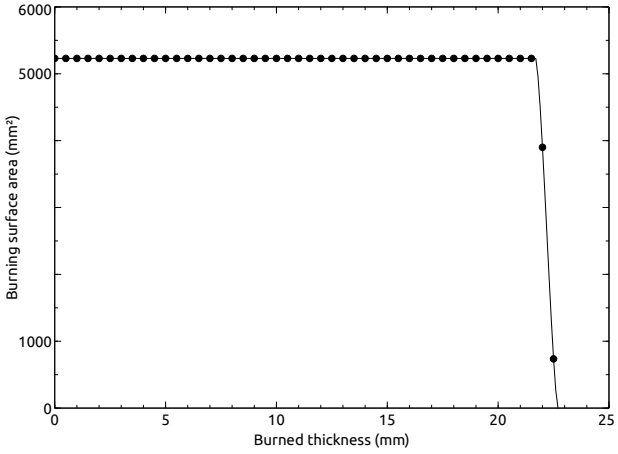

Figure 9: Reconstructed burning surface evolution

The experimentally measured chamber pressure $\bar{P}$ is equal to 1.22 Mpa just after the ignition while the initial burning surface is equal to 5230 mm^2. Then, if we convert the curve in figure 9 by dividing the burned thickness by 6.14 (and shifting it by 0.37 to correct for the ignition delay) to get the time and multiply the burning surface by $\frac{1.22}{5230}$ to scale the first point to the chamber pressure we find the fat gray curve in figure 10.

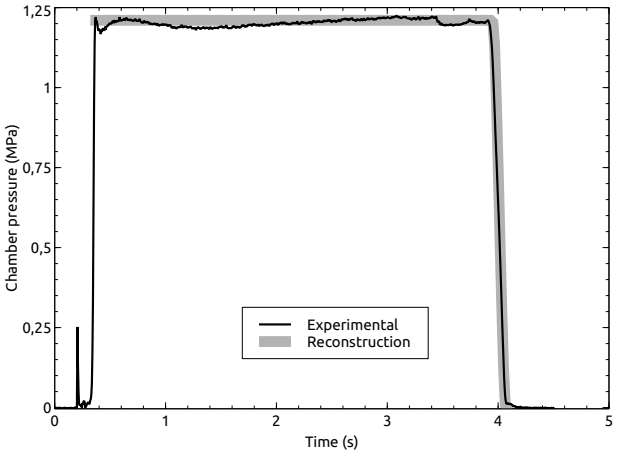

Figure 10: Fitting with experimental Pressure

We note that, despite some pressure fluctuations during the run than can not be captured by a purely geometrical regression, the slope of the pressure curve at the end of the burn and the duration of the burn are almost perfectly captured.

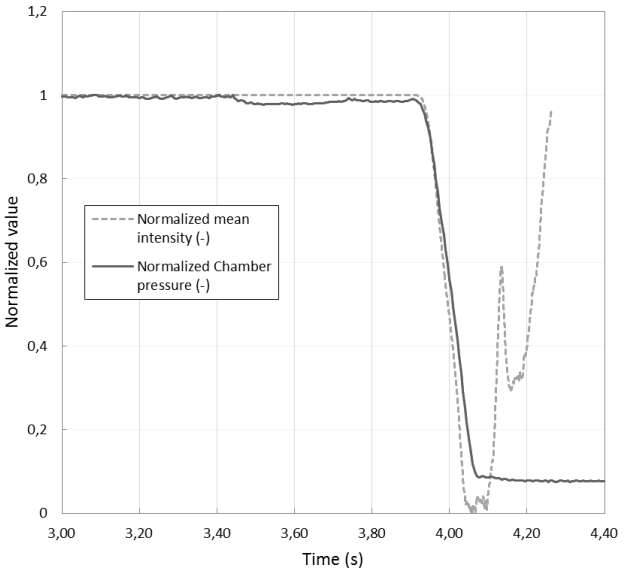

Figure 11: Light intesity vs. chamber pressure

For the second method mentioned in 3.1 we compare the (arbitrarily normalised with the value at t=3.0 s) values of the chamber pressure $\bar{P}$ and the average light intensity for each frame. Figure 11 shows a very nice overall agreement. There is a slight drop in pressure after 3.45 s that we see in other LP8 experiments but that we can not explain for the moment.

4.3 LP8#11

The only difference between LP8#03 and LP8#11 is the voluntarily increased charge for the igniter.

Figure 12 shows the different phases of the burn as seen by the high speed camera and correlated to the pressure curve. We clearly see the influence of the modification to the igniter in both the over-pressure during the first second and the gradual pressure reduction at the end of the run (cf. figure 8 for comparison). In the image referred to as “First trace of hyperbole” we distinctly see the trace of the furrow caused by the beefed up igniter. However, given the ad-hoc nature of these tests we used very old propellant grains. This can be seen in the bright circles appearing at the end of the burn. These circles are probably due to the migrating of the different components (basically ammonium perchlorate) to the surface of the grain causing inhomogeneities that, locally, change the regression rate. These bright spots make it difficult to follow the trace of the initial furrow created by the igniter.

It seems defensible to assume that the igniter digs deeper into the surface close to its nozzle while the influence becomes less further away. This leads to a first, simple, assumption that the initial furrow is conical in shape (see figure 13 for the definitions with the origin of the coordinate system at the centre of the base of the cone) and can be written as:

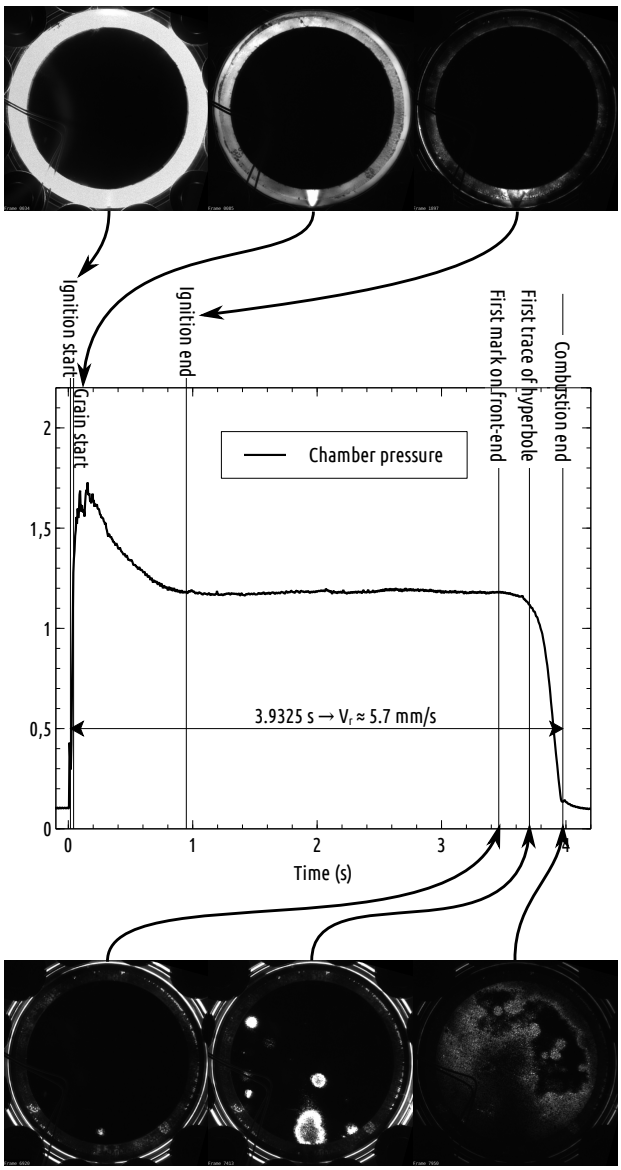

Figure 12: Correlation between HS video and pressure measurements

$$x^2 + z^2 = r^2(y) \tag{1}$$

$$\text{where } r(y) = R - \tan(\alpha) \times y \tag{2}$$

Now, if the regression rate is constant everywhere, then the trace of the furrow on the plane $z = H$ (the front end filmed by the HS camera) for $R > H$ is given by:

$$y = \frac{R - \sqrt{x^2 + H^2}}{\tan(\alpha)} \tag{3}$$

Using the data given in figure 12 we find the following:

	frame	time (s)
Ignition	34	0.0170
Grain start	85	0.0425
Igniter end	1897	0.9485
First mark on front-end	6920	3.4600
First trace of hyperbole	7413	3.7065
Combustion end	7950	3.9750

Table 1: timing of the diferent phases of the run

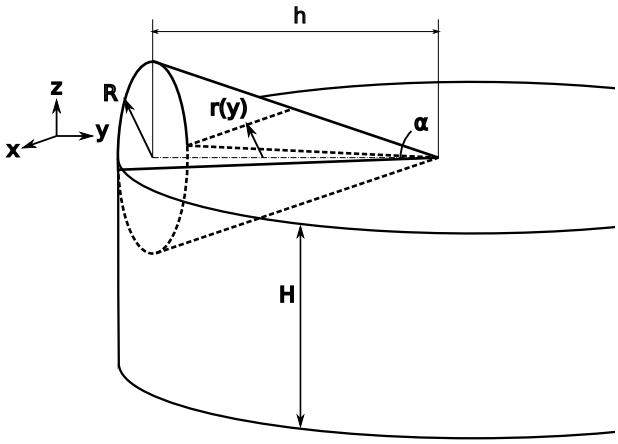

Figure 13: Definition of the conical furrow

To avoid the bias of human interpretation, an attempt was made to design a tracking algorithm to follow the contour of the initial cone on the surface of the head-end. However, the bright circles appearing on or close to the contour make this approach very error prone. As shown in figure 14, we find that $\alpha \approx 4°$ and almost constant over time as expected. However, we see that $R \approx -20.82 + 11.93 \times t$ so that $\bar{V}_r = \frac{dR}{dt} \approx 11.93$ mm/s. This is more than twice the experimental value of $\bar{V}_r$.

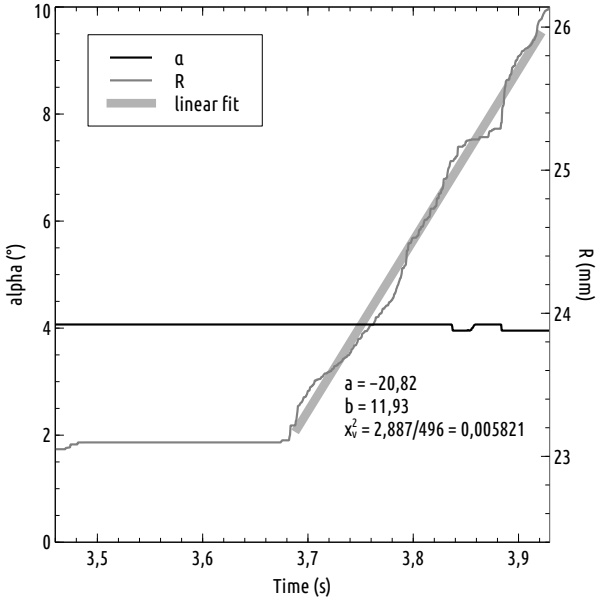

Figure 14: Front tracking algorithm, first attempt

As an alternative approach we take a frame from the HS footage where the trace is well captured (little influence from the bright spots mentioned earlier) we can get an estimation of the value of α, that remains unchanged during the run, and the value of $R(t)$ (see equation 3).

Frame number 7640 (t=3.82 s) is such a frame (see figure 15) and with the values for $\Delta x = 20.6\ mm$ and $\Delta y = 27.4\ mm$ we find the following values for α and $R(t)$:

$$y := 0 \rightarrow R(3.28) = \sqrt{\left(\frac{\Delta x}{2}\right)^2 + H^2} \approx 24.7\ mm \quad (4)$$

$$x := 0 \rightarrow \alpha = \tan^{-1}\left(\frac{R - H}{\Delta y}\right) \approx 4.7° \quad (5)$$

Now, if we use these values to reconstruct the burning surface evolution and fit it to the experimental data (as we did in section 3.2), we find the curve given in figure 16. We notice that the moment the head-end starts to uncover is nicely captured but the evolution after this point is a bit off. This is probably due to the same inhomogeneous propellant that caused the bright circles.

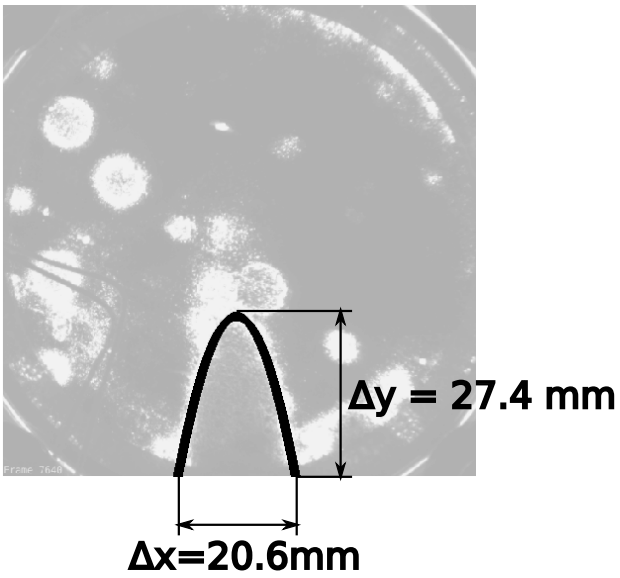

Figure 15: Hyperbole fitting

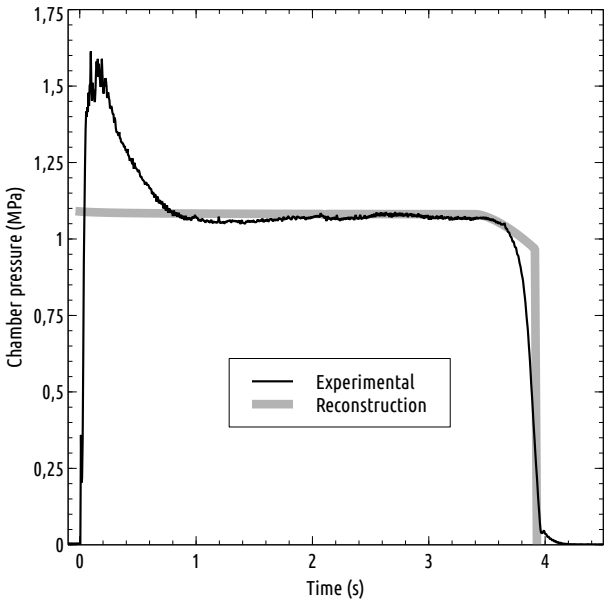

Figure 16: fitting experimental pressure with surface area

5 Conclusions

In order to investigate the influence of the pyrotechnical igniter on the topology of the burning surface of a “cigaret”

burning, small scale engine, an innovative method has been developed. An existing, experimental, set-up has been equipped with a transparent head-end. A high-speed camera captures the final instances of the test run as the burning surface “hits” the head-end.

The captured flame propagation reveals the position of the interface between the head-end and the burning surface. The evolution of this interface allows us to reconstruct the topology of the burning surface just before the extinction of the engine. The whole test run can then be reconstructed by offsetting a smoothed approximation of this topology with the inverted, average, regression rate $\bar{V}_r$.

The method has been applied to the measurements of two test firings with respectively a weak and a strong igniter charge.

For the weak igniter charge, the topology of the burning surface is rather flat and a least square method works extremely well to define the best fitting plane. However, for the strong igniter charge the surface is not flat and the reconstruction is a lot harder. An attempt was made to device a tracking algorithm to avoid the bias induced by human interpretation. Due to the exploratory nature of this study old, left over, propellant grains were used. The components of these grains have segregated leading to a lot of noise in the captured images (bright circles) that fooled our tracking algorithm in following the wrong contours. A manual approach based on frames where the contour is clearly visible gave excellent results.

The next step is to repeat the experiment with the strong igniter charge and a fresh propellant grain to improve the tracing algorithm and render the method more reproducible and avoid human interpretation and its inherent bias.